

The evolution of texture in thin films and multilayers via synchrotron transmission Laue and grazing-incidence x-ray scattering

J C Bilello†, S M Yalisove† and Z U Rek‡

† Department of Materials Science and Engineering, University of Michigan, Ann Arbor, MI 48109-2136, USA

‡ Stanford Synchrotron Radiation Laboratory, SLAC Bin 69, Box 4349, Stanford, CA 94309, USA

Received 5 September 1994, in final form 23 November 1994

Abstract. Sputter-deposited films and multilayers are used for a wide variety of applications including protective coatings on turbine engine blades, magnetic recording heads, optical elements, electronic packaging, x-ray filters and monochromator components to name a few examples. This wide range of interest requires growth thicknesses from a few nanometres to tens of micrometres depending on the product. In many applications, specific film textures in the growth direction as well as in the plane of growth are required. The control and manipulation of these textures can be accomplished by using advanced characterization techniques to select particular processing conditions. A variety of x-ray methods including grazing-incidence x-ray scattering, conventional pole figure studies and synchrotron white-beam transmission Laue scattering were used to study texture evolution for the thinnest films up to the thickest multilayer coatings.

1. Introduction

The microstructure of thin films and multilayers plays a critical role in determining the optimization of the physical properties of interest. Variations in the film processing parameters that are responsible for the ultimate morphology of the microstructure have been described in terms of a zone scheme, which has been discussed in the well-known review article by Thornton [1]. The texture of a given film, or multilayer, is a more subtle feature of the microstructure and has important consequences in determining ultimate film properties [2–5]. Recent observations have shown that films grown in the same system can exhibit different textures depending on the exact deposition conditions [6]. These films were observed to have nearly equivalent columnar grain size and distribution. It has also been found that, in growing large-scale multilayer–multiscalar microlaminates, texture can play an important part in governing the mechanical anisotropy. In the case of these multi-scalar microlaminates, up to 1500 layers (with layer thicknesses from 4 nm to 5 μm) were assembled into multilayer sheets of 30–60 μm total thickness by 75 mm in diameter, producing microlaminates with both strength and toughness [7, 8].

However, controlling the anisotropy of such a complex material requires assessing both the texture normal to the growth plane (*out-of-plane*) and that lying in the plane of deposition (*in-plane*) over a length scale that varied from a few tens of nanometres to tens of micrometres. No single technique is available that is capable of delivering texture information over this scale range. In order to perform our observations, conventional pole figure analysis was combined with new techniques, which determined partial pole figures for the very thinnest films using a grazing-incidence x-ray scattering (GIXS) configuration. For the thickest films, and multilayers, synchrotron white-beam transmission Laue (WBTL) scattering was employed [9, 10].

2. Experimental

2.1. Sample preparation

Thin film and multilayer sputter deposition has been reported elsewhere and hence only a brief outline of the sample preparation will be given here [6, 7]. Refractory metal Mo and W targets 150 mm in diameter were

used in a cryopumped DC and RF magnetron sputter-deposition system. Deposition rates of 35–67 nm min⁻¹ were employed. All films were deposited on ‘as-received’ Si(100) substrates onto the native oxide. Film thicknesses were measured with a DEKTAK stylus profilometer calibrated by Rutherford backscattering spectroscopy and cross section transmission electron microscopy.

2.2. Conventional pole figures

Preferred orientations were measured using a Rigaku automated texture diffractometer in the Schulz geometry [11]. This camera was used on a 12 kW Rigaku rotating anode x-ray generator equipped with a Cu K α target. Pole figures for the Mo (110), (200) and (211) reflections were obtained and plotted quantitatively using the standard ‘times random’ method [12]. The intensities obtained in the thin-film pole figures were normalized by using a well-annealed bulk polycrystalline Mo sample, which had a measured random grain size of about 10 μ m. All pole figures were taken in the reflection mode. In practice, data from samples thinner than about 100 nm did not yield meaningful results because the small sample volume produced such low count rates. This resulted in long data collection times as well as poor resolution due to low signal-to-noise ratios. In addition, the limited collimation and relatively broad divergence of the laboratory source made it difficult to limit the strong signal from the Si substrates. Background scattering from the substrate enhances the difficulty of obtaining sufficient diffracted intensity from very thin Mo films. It should also be noted that the upper end of the thickness range for obtaining conventional pole figures was about 3 μ m, namely about half the extinction distance for Mo.

2.3. Texture analysis via grazing-angle incidence scattering

All GIXS experiments were carried out at the Stanford Synchrotron Radiation Laboratory (SSRL) on the wiggler beamline 7-2 with the monochromator set at 10 keV. Figure 1 shows the experimental set-up for obtaining partial-pole figures in the GIXS mode. In this configuration the incident beam I_0 impinges on the sample wafer at an angle α , which was varied in the range 0.15–1.5° to depth-profile the Mo surface coating while virtually ignoring signal from the substrate. Since the critical angle for total reflectance at 100 keV incidence, beam energy for Mo is about 0.347°, the penetration of x-rays into the substrate is small when α is less than the critical angle for Mo, that is, scattering comes from a very thin layer of Mo but most of the beam was reflected from the Si substrate. This virtually eliminated substrate scattering and enormously improved signal-to-noise level; however, the price was very long data collection times even on a wiggler beam line. Complete ϕ scans for one diffracted (hkl), at one depth, took 1–2 h for the thinnest films. The term

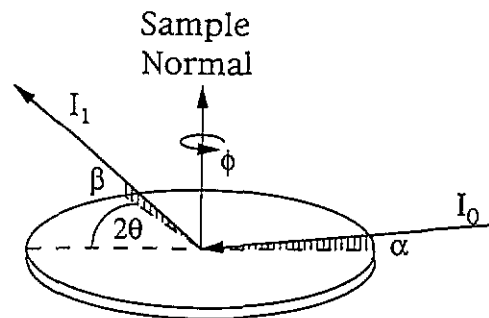


Figure 1. The grazing-incidence geometry for obtaining partial pole figures of very thin films.

‘partial’ is used in the sense that the GIXS mode scans reflecting planes in the film that are nearly perpendicular to the surface of the substrate, so a complete analysis of *all* reflecting planes of the same $\{hkl\}$ family is not possible, as would be the case with conventional pole figure data taken from thick samples. The incident and scattering angles, α and β respectively, were set equal. The detector was arranged to collect the scattered intensity I_1 from a particular (hkl) Bragg peak, that at 2θ . Once this had been done, the sample was rotated a full $\phi = 360^\circ$ about the sample normal axis to detect the variation in intensity as a function of ϕ , as shown in figure 1. For a random sample one would expect uniform intensity, namely I_1 constant as ϕ goes from 0 to 360° . Conversely, any localization in intensity would indicate some preferred orientation. However, one must apply the caution that this method does not scan all the planes of an $\{hkl\}$ zone, but only indicates the degree of texture of those planes that are nearly perpendicular to the growth surface.

2.4. Synchrotron white-beam transmission Laue scattering

Examination of polycrystalline thick films and multilayers was most readily performed using the WBTL mode [13]. This method is usually employed to study bulk defects in solids or to orient single crystals, but in the present case defect resolution is not the issue; instead the wavelength (or energy) distribution of the incident beam is used to detect an angular spread of either strain or orientation in the sample. By using various pre-filters, the incident beam energy was truncated to allow one to probe a well-defined region of reciprocal space and more readily identify the reflections and corresponding angular scattering range, which coincided with any preferred orientation. The set-up for WBTL is straightforward and has been discussed in many references to which the reader is referred [14, 15].

2.5. Transmission electron microscopy

Plan-view transmission electron microscopy (TEM) and transmission electron diffraction (TED) were performed on samples prepared from the sputtered Mo films. These samples were ultrasonically cut into 3 mm discs, mechanically thinned from the back side (the Si

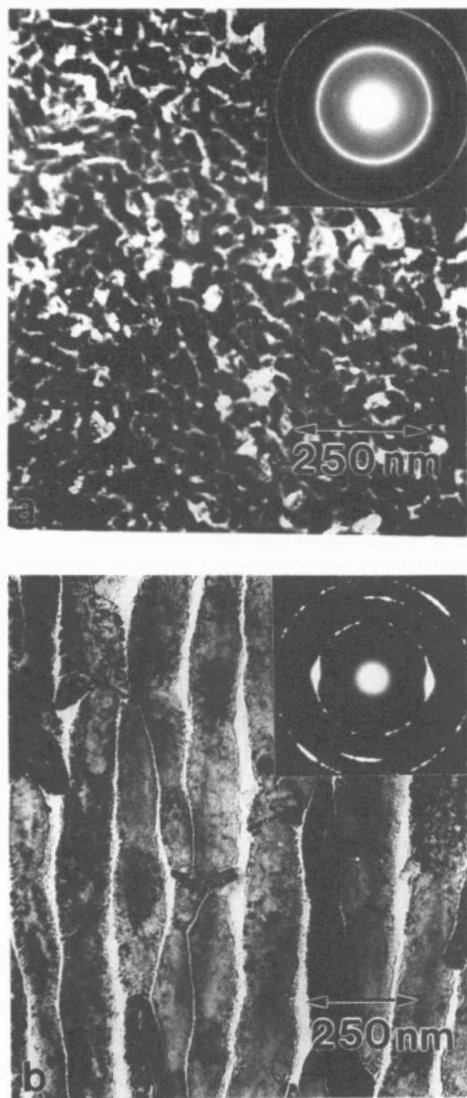


Figure 2. Plan-view transmission electron microscopy and diffraction (insets in the upper left-hand corners of the micrographs) of Mo films deposited on a Si(100) 75 mm diameter 'as-received' wafer: (a) 200 nm and (b) 2 μm thick.

substrate), and chemically etched to perforation with a $\text{HNO}_3\text{-HF-CH}_3\text{COOH}$ mixture. Because the samples were thinned and etched from the back side, while protecting the film surface, the area examined was the top 100–1000 Å of the deposited film. The TEM analysis was carried out on a Philips 420 T electron microscope, operated at 120 kV.

3. Results and discussion

Randomly distributed, equiaxial grains were observed in the thinnest films. For thicker films, columnar grains with strong preferred orientation evolved. The qualitative aspects of this observation can be readily seen in figure 2, which was typical of many samples that were studied. Here in figure 2(a) the 200 nm film shows a fine grain size, which is nearly randomly distributed as indicated by the rather uniform Debye rings obtained, as

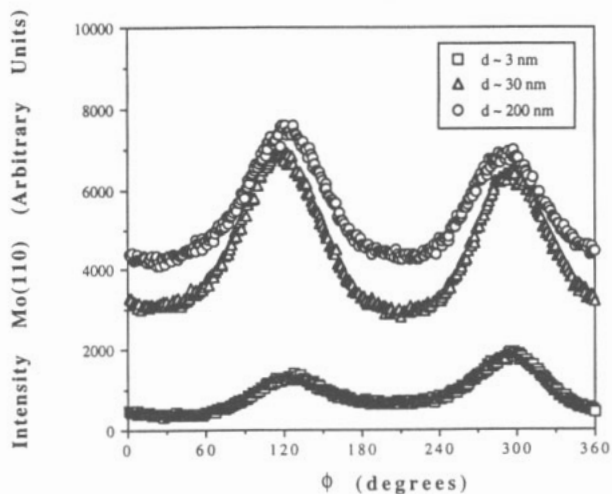


Figure 3. A grazing-incidence x-ray scattering ϕ scan from 0 to 360° about the sample normal of the Mo(110) Bragg peak for a 200 nm thick Mo film. The depth, d , is measured from the free surface of the film. Similar results were found for the (200) and (211) reflections.

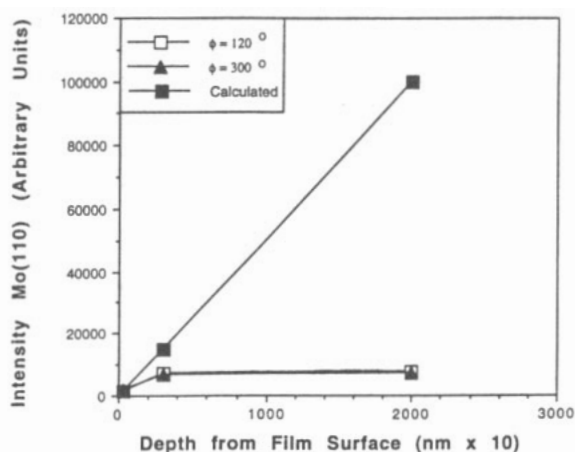


Figure 4. A comparison of the Mo(110) diffracted intensity as a function of depth with the theoretical value for a fully developed texture. Similar results were found for the (200) and (211) reflections.

shown on the inset TED. As the film thickness increased to 2 μm , eventually a columnar grain pattern evolved and a strong preferred orientation developed, as indicated by the TED shown on inset figure 2(b). These grains have their long axes in the growth direction and extend almost the full thickness of the film. The following questions arise. **When does this preferred orientation develop** and can one obtain more quantitative information on the extent and degree of texture that is not easy to verify via TEM? To clarify this texture evolution, experiments focused on observations scaling from the thinnest films to the thickest, using in turn GIXS, conventional pole figures and finally WBTL analysis.

3.1. Grazing-incidence x-ray scattering observations

Figure 3 shows ϕ scans of the Mo(110) Bragg peak taken in the GIXS mode with incident beam angles $\alpha = 0.30$, 0.37 and 1.50 corresponding to the depths $d = 3$, 30 and 200 nm (full film thickness), respectively. Similar

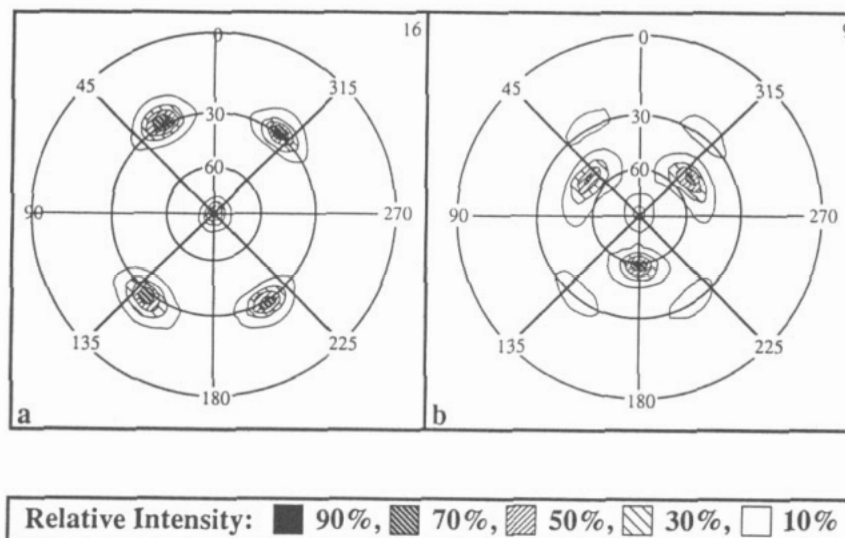


Figure 5. The (110) pole figures for samples grown under two different types of processing conditions. The sample normal coincides with the normal to the pole figure. The (200) and (211) pole figures showed similar results, but are omitted for the sake of brevity. (a) A 2 μm thick Mo film grown under dynamic conditions with 34 nm min^{-1} deposition rate shows a (110) *out-of-plane* and a (110) *in-plane* preferred orientation. (b) A 2 μm thick Mo film grown under dynamic conditions with a 67 nm min^{-1} deposition rate shows a (110) *out-of-plane*, but a (111)–(110) *in-plane*, preferred orientation.

data were taken for the Mo(200) and (211) reflections. Distinct maxima in the intensity were found at about 120° and 300° for Mo(110) scattering. Similar scans for Mo(110), (200) and (211) were taken for an 80 nm film (not shown) and no maxima as a function of ϕ were found, but only a flat intensity distribution over the full $360^\circ\phi$ scan range.

One can get an approximate idea of the degree of texture at each depth by assuming that the segment of the film furthest from the film–substrate interface had the highest degree of texture. The diffracted intensity from that volume could then be compared with the ideal case of a film with a more fully developed texture. If the sample segment were perfectly aligned in the growth direction then the scattering would be that of an oriented single crystal. The signal would diminish for an *ideal* polycrystal texture because of the mosaic spread. In practice one can estimate the so-called *ideal* texture from comparisons with the random polycrystalline sample. However, it is clear from the TEM observations that the grain size and mosaic spread is much smaller in the thin film. Using these ideas one can estimate that the 200 nm film scan to a depth $d = 3$ nm is nearly 100% textured. This, of course, is only a rough estimate and the spread in the calculated degree of texture at the 3 nm depth layer from the surface is large, being 70–100%. Nevertheless, the remaining depth profile should scale directly as the scattering volume of the particular layer compared with the scattering intensity of the surface layer. The results are plotted in figure 4 and show that most of the texture has evolved in the upper 30 nm of the film, namely 170 nm from the growth interface.

3.2. Conventional pole figure analysis

For thicker samples ($\geq 0.5 \mu\text{m}$) reflection pole figure analysis is simple, straightforward and provides information over the volume of the full sample down to about half the extinction depth. As Mo films are deposited to a thickness of 2 μm , texture develops not only in the growth direction (*out-of-plane*), but also the grains of the film develop a preferred orientation within the plane of growth (*in-plane*). While the former type of film texture is well known the latter has received less attention [6]. Figure 5 shows pole figures taken on 2 μm thick Mo grown under nearly identical conditions, except for the deposition rate. In the first case, figure 5(a), the sample was deposited at 34 nm min^{-1} . In the latter case, illustrated in figure 5(b), the sample was grown at 67 nm min^{-1} (both of these were deposited onto moving substrates, that is the substrates were mounted on a platen that rotated past the source at 20 rpm, and this was designated, in general, as dynamic growth). In the slow dynamical growth case, a strong (110) *out-of-plane* texture is observed and is consistent with the GIXS experiments. In this case a distinct (110) *in-plane* texture is also observed. This *in-plane* texture would have been difficult to confirm in the GIXS mode because {110} planes inclined to the surface needed to be scanned and not all these are accessible in the grazing-incidence setting (as pointed out above).

3.3. Laue textures

To study the texture of thick films and multilayers of Mo and Mo/W, respectively, it was found that WBTL

4. Conclusions

The present work has demonstrated that a variety of techniques can provide information on the evolution of texture in sputter-deposited films and multilayers over a thickness depth range that varied from a few tens of nanometres to a few tens of micrometres. These techniques included grazing-incidence x-ray scattering, plan-view transmission electron microscopy, transmission electron diffraction, conventional laboratory source pole-figure diffractometry and WBTL. No single method is capable of spanning the entire range of interest in producing large-scale multilayers and thick monolithic film coatings. The two synchrotron methods, namely GIXS and WBTL, are especially useful for the thinnest and thickest cases, respectively. They have the advantage of being non-destructive so that sample preparation is simple and the volume of examination can readily be identified.

The GIXS observations, correlated with the TEM and TED ones, on the thinner samples indicated that a critical thickness was required before texture started to develop. In the case of the monolithic Mo films, these conditions occurred over the range 80–170 nm. Film growth is naturally a sensitive function of processing conditions, so this range needs to be explored in much more detail to understand the mechanism whereby a film of approximately random nuclei develops both *in-plane* and *out-of-plane* textures when a critical thickness range is reached. The theory in the latter (*out-of-plane*) case has received some consideration in the literature [17, 18], but the former case of *in-plane* texture has received much less attention. This critical thickness effect can have important consequences in certain applications in which film anisotropy is an important design parameter.

Finally, the evolution of the texture can be modified by controlling the growth conditions. This has been demonstrated in the case of Mo films for dynamic depositions using different growth rates and the present WBTL observations confirm that this persists as the film thickness increases to the level of micrometres.

Acknowledgments

This research was supported by ARO and ARPA under contract DAAL03-91-G-0235 with synchrotron radiation studies performed at Stanford Synchrotron Radiation Laboratories, supported by the USA's DoE. Thanks are also due to O P Karpenko and M Vill of the University of Michigan for their assistance in carrying out this work.

References

- [1] Thornton J A 1977 *Ann. Rev. Mater. Sci.* **7** 239
- [2] Pennelle R 1978 *Texture of Materials* ed G Gottstein and K Lücke (New York: Springer) pp 129–53
- [3] Knorr D B, Tracy D P and Robell K P 1991 *Appl. Phys. Lett.* **59** 3241
- [4] Campbell A N, Mikawa R E and Knorr D B 1993 *J. Electron. Mater.* **22** 589
- [5] Kief M T and Egelhoff W F Jr 1993 *J. Appl. Phys.* **73** 6195
- [6] Karpenko O P, Bilello J C and Yalisove S M 1994 *J. Appl. Phys.* **76** 4610
- [7] Vill M, Adams D P, Yalisove S M and Bilello J C 1993 *Mater. Res. Soc. Symp. Proc.* **308** 759
- [8] Adams D P, Vill M, Tao J, Bilello J C and Yalisove S M 1993 *J. Appl. Phys.* **74** 1015
- [9] Karpenko O P, Vill M, Malhotra S G, Bilello J C, Yalisove S M and Rek Z U 1993 Activity report (Stanford Synchrotron Radiation Laboratory) pp 116–18
- [10] Vill M, Rek Z U, Malhotra S G, Yalisove S M and Bilello J C 1993 Activity report (Stanford Synchrotron Radiation Laboratory) pp 123–6
- [11] Schultz L G 1949 *J. Appl. Phys.* **20** 1030
- [12] Barrett C S 1952 *Structure of Metals* (New York: McGraw-Hill) pp 442–518
- [13] Tanner B K 1976 *X-ray Diffraction Topography* (Oxford: Pergamon) pp 25, 56–9
- [14] Bilello J C, Chen H, Hmelo A B, Liu J M, Birnbaum H K, Herley P J and Green R E Jr 1983 *Nucl. Instrum. Methods* **215** 291
- [15] Stock S R, Chang Y H, Chang P C, Rek Z U and Ditchek B M 1993 *J. Appl. Phys.* **73** 1737
- [16] Vill M, Adams D P, Yalisove S M and Bilello J C 1994 *Acta Met. Mater.* to be published
- [17] Srolovitz D J 1986 *J. Vac. Sci. Technol. A* **4** 2925
- [18] Srolovitz D J, Mazor A and Bukiet B G 1988 *J. Vac. Sci. Technol. A* **6** 2371